

## Chapter 3

# Sample Description

The samples analyzed in this study consist of eleven CAIs, of which eight belong to Efremovka and three to Grosnaja meteorite. These samples were studied for their petrographic and chemical composition at the Vernadsky Institute, Moscow, Russia. The inclusions were classified following the petrographic criteria suggested by Grossman (1975, 1980) and Wark and Lovering (1977); this is given in Table 3.1. One of the most important features of the Efremovka CAIs is that they do not show any signature of major secondary petrographic alteration (Ulyanov et al. 1982) attesting to their pristine preservation. This is not the case for Grosnaja CAIs which show distinct signatures of petrographic alteration (Ulyanov 91, Goswami et al., 1993). The documentation of the inclusions were carried out by an electron probe (Cameca Camebax), a scanning electron microscope (Cambridge S4/10) equipped with an energy dispersive X-ray analyzer and a Carl Zeiss optical microscope. The chemical composition of the different primary and secondary phases observed in the CAIs is given in Table 3.2. A brief description of individual CAIs is given below and the elemental composition of individual CAIs is given in Tables 3.3-3.6.

### 3.1 Efremovka CAIs

**E2, E59 :** These are compact type A inclusions. E2 which measures  $\sim 2$  cm is one of the largest CAIs seen in Efremovka and E59 (Fig. 3.1a) is  $\sim 1$ cm across. The major mineral

phase in these inclusions are melilite (~ 75%) and spinels (17%) and some minor phases (pervoskite ~3%, Fe-Ni metal ~ 0.4%). Fassaite also occurs as a minor phase in these CAIs. These inclusions have a thick multilayered rim with layer sequence similar to type B1 CAIs (described below). The Akermanite content of melilite in the near rim region is ~ 10 mole % but steadily increases to ~ 35% as one moves to the inclusion interior. Petrographic description of E2 is given by Ulyanov et al. (1982) and Fahey et al. (1987b). This CAI has also been analyzed for REE and oxygen isotopic compositions (Ulyanov et al., 1982, 1988; Nazarov et al., 1982, 1984). Additional REE and Mg isotopic compositions have been reported by Fahey et al. (1987b).

**E40, E44, E65 :** These are type B1 CAIs (E40: Fig 3.1b; E44: Fig 3.1c and E65 Fig 3.1d) which mainly consist of a melilite mantle and a pyroxene rich core. All the inclusions have a 20 to 30 $\mu$ m thick multilayered rim with a layer sequence of (as one moves outward from the inclusion) spinel ( $\pm$  perovskite), melilite, and an outer layer of pyroxene that is zoned from Ti-Al-rich fassaite to aluminous diopside. Hibonite is also present in some of the spinel-melilite layer of E40 rim. The spinel grains in the interior of E40 are relatively large ( up to about ~ 100 $\mu$ m in the core). The spinel grains are in general isometric crystals that are poikilitically enclosed by pyroxenes and melilite. They are extremely pure and their TiO<sub>2</sub> and FeO content is < 1%. Metal grains and anorthite are generally present in the core region although some times they are also present in the mantle. The abundance of Fe-Ni metal decreases from E65 to E40 to E44.

The pyroxenes in these inclusions show variations in their TiO<sub>2</sub> content from 2.5% in E65 to ~ 14.5% in E40 (Table 3.4). The pyroxenes are zoned; the smaller ones show simple zoning (Ti-rich core and Ti-poor rim) and the larger ones show complex zoning. The compositional data and stoichiometric considerations suggest that a good fraction of Ti in these inclusions is present in the trivalent state. Melilite in all the inclusions show compositional zoning with the core being rich in akermanite content (55-70 mole%) while it decreases in the near rim region (10-30 mole%) (Table 3.3). Mineralogical studies of inclusions E40 and E65 have been carried out by Ulyanov and Kononkova (1990). The REE

composition of E40 was measured by Ulyanov and Kolesov (1984), and oxygen isotopic compositions of bulk samples of E40 were communicated by Ulyanov et al. (1988).

**E50 :** It is a large (~ 1cm) multizoned hibonite-rich inclusion (Fig. 3.1e) containing a melilite-perovskite zone, a melilite-spinel zone, a melilite-spinel perovskite zone and the hibonite rich zone. Small ( $\leq 10\mu\text{m}$ ) perovskite grains are extremely abundant in the melilite-perovskite zone. In the interior of the inclusion, where an association of melilite and perovskite is observed, the perovskites are slightly larger. The spinel grains are small and are poikilitically enclosed by the melilite. In the hibonite-rich zone, the hibonite has a lath like structure, and the spinel grains present in this zone are interwoven with melilite. The elemental composition of different mineral phases of E50 is given in Table 3.5.

**E36, E60 :** These are type B2 CAIs, E36 is a small inclusion (~ 5mm) across (Fig. 3.1f) while E60 is larger ~ 1cm across (Fig 3.1g). These inclusions have large melilite and pyroxene grains with smaller spinel grains enclosed in them. The pyroxene composition in E60 is similar to that of type B1 inclusions (Table 3.4). The melilite composition is highly akermanitic except near the outer edge (Table 3.3). There are a couple of localized spots in E60 where the presence of nepheline suggest minor low temperature alteration. There is a single layer diopside rim around the inclusions. The oxygen isotopic compositions of bulk sample of E60, and its mineral separates were reported by Ulyanov et al. (1988).

## 3.2 Grosnaja CAIs

**GR4 :** It is a type A inclusion, ~ 1mm across, and is predominantly composed of melilite (Fig. 3.1h). There are very few spinel grains in the interior of this CAI. The rim does not exhibit distinct layered structure. Secondary alteration products (garnet, Fe-rich olivine and Na-rich plagioclase) are present in some localized areas near the rim region. The average major element composition of the different mineral phases are given in Table 3.6.

**GR2 :** It is the only Type C inclusion analyzed in this work and is ~ 2mm across (Fig. 3.1i). It mainly consists of anorthite and pyroxene and its structure indicates that it has

probably originated from a melt. The chemical composition of different mineral phases is given in Table 3.6. The pyroxenes in the core have higher Al and lower Mg content compared to mantle pyroxenes. The TiO<sub>2</sub> content of the core pyroxenes is higher than the mantle pyroxenes. This inclusion has secondary alteration phases near the rim which mainly comprises of garnets, calcite, Na-rich plagioclase.

**GR7:** This is the largest inclusion from Grosnaja meteorite analyzed in this work and is ~ 1cm across (Fig. 3.1j). It belongs to the type B petrographic class. It is mainly composed of melilite with occasional pyroxenes. The REE data show a pattern that is similar to Group VI with enrichment in Eu and Yb. Melilite composition shows a broad range of akermanite content (15-55 mole%).

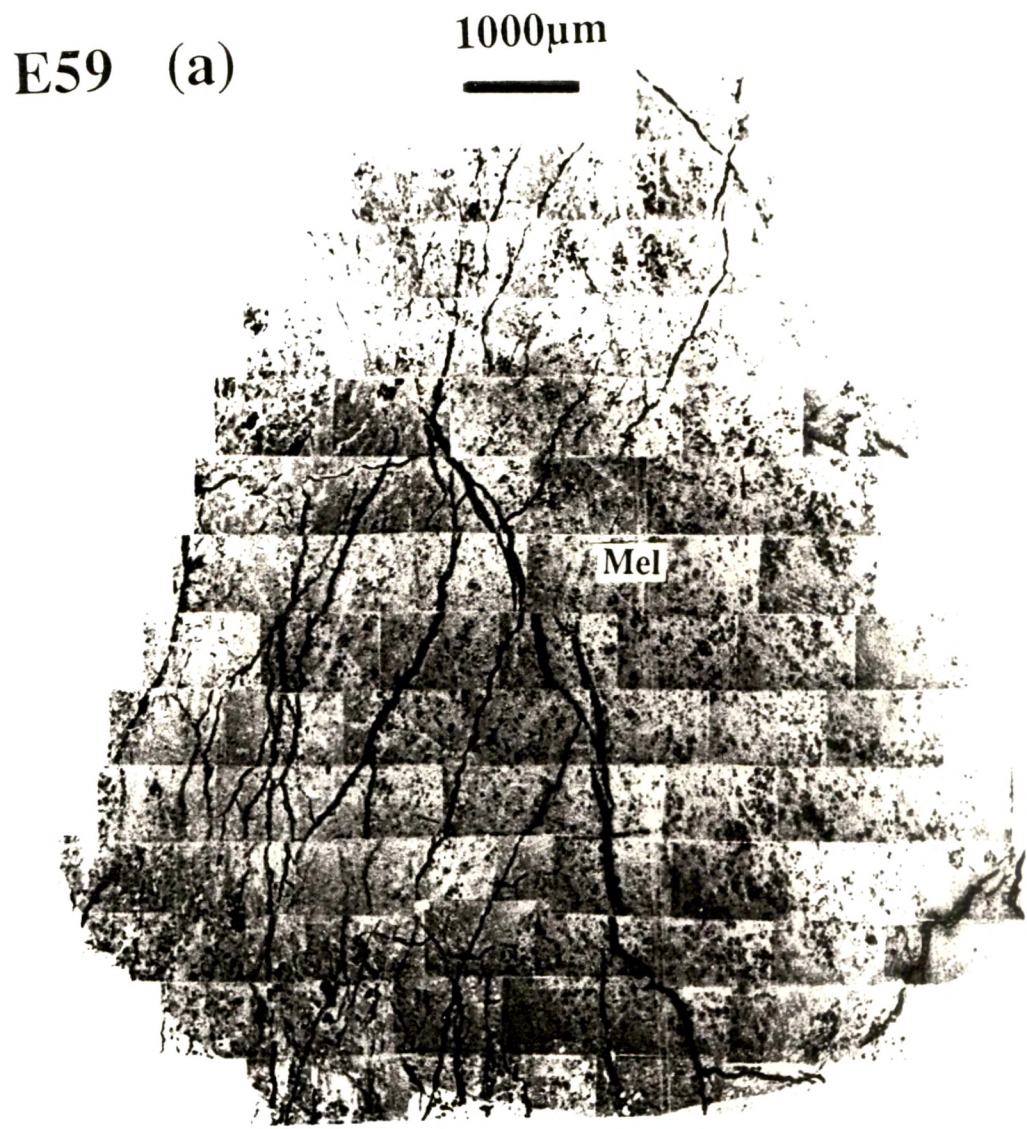


Fig.3.1

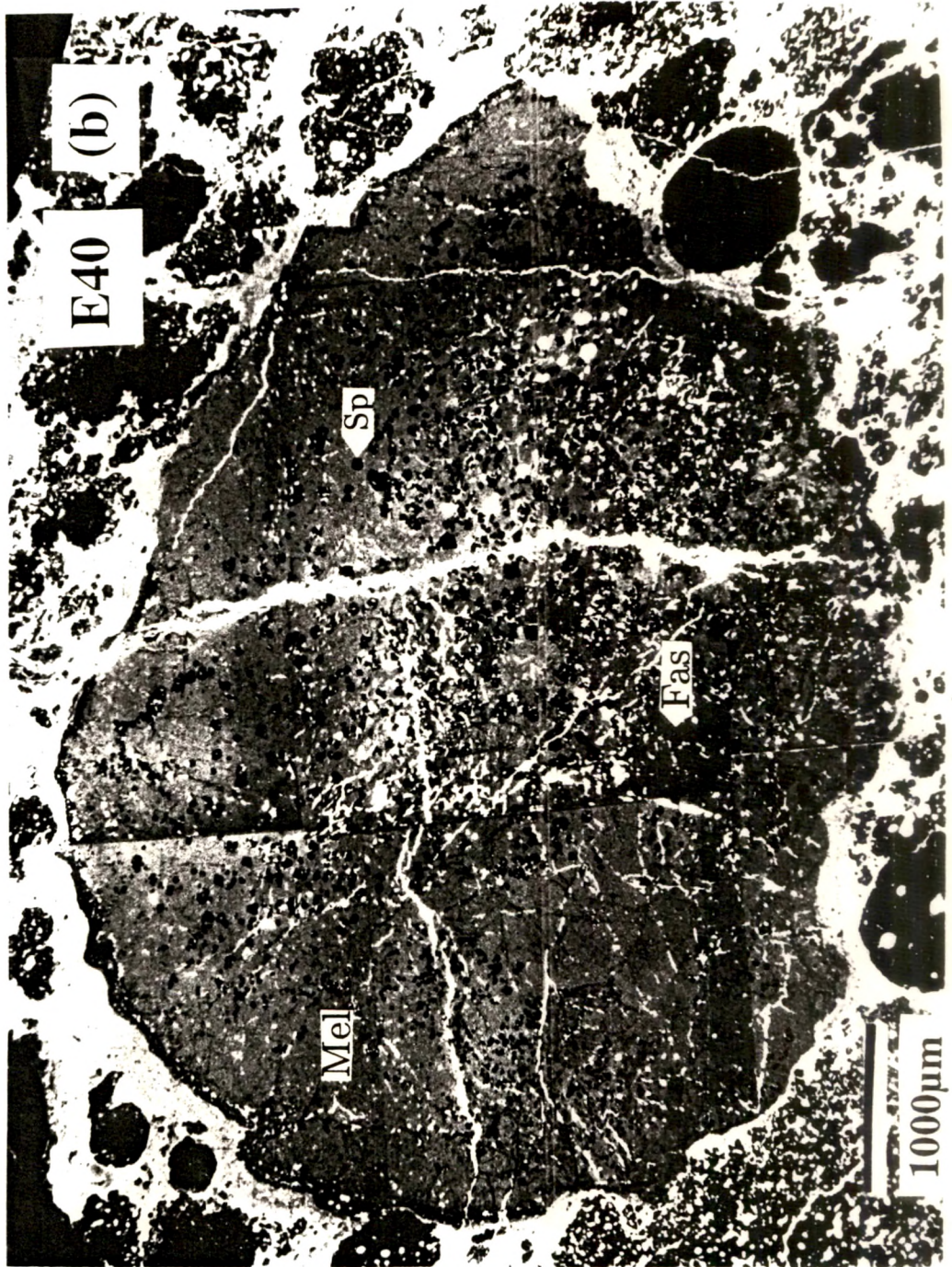


Fig.3.1 (Continued)

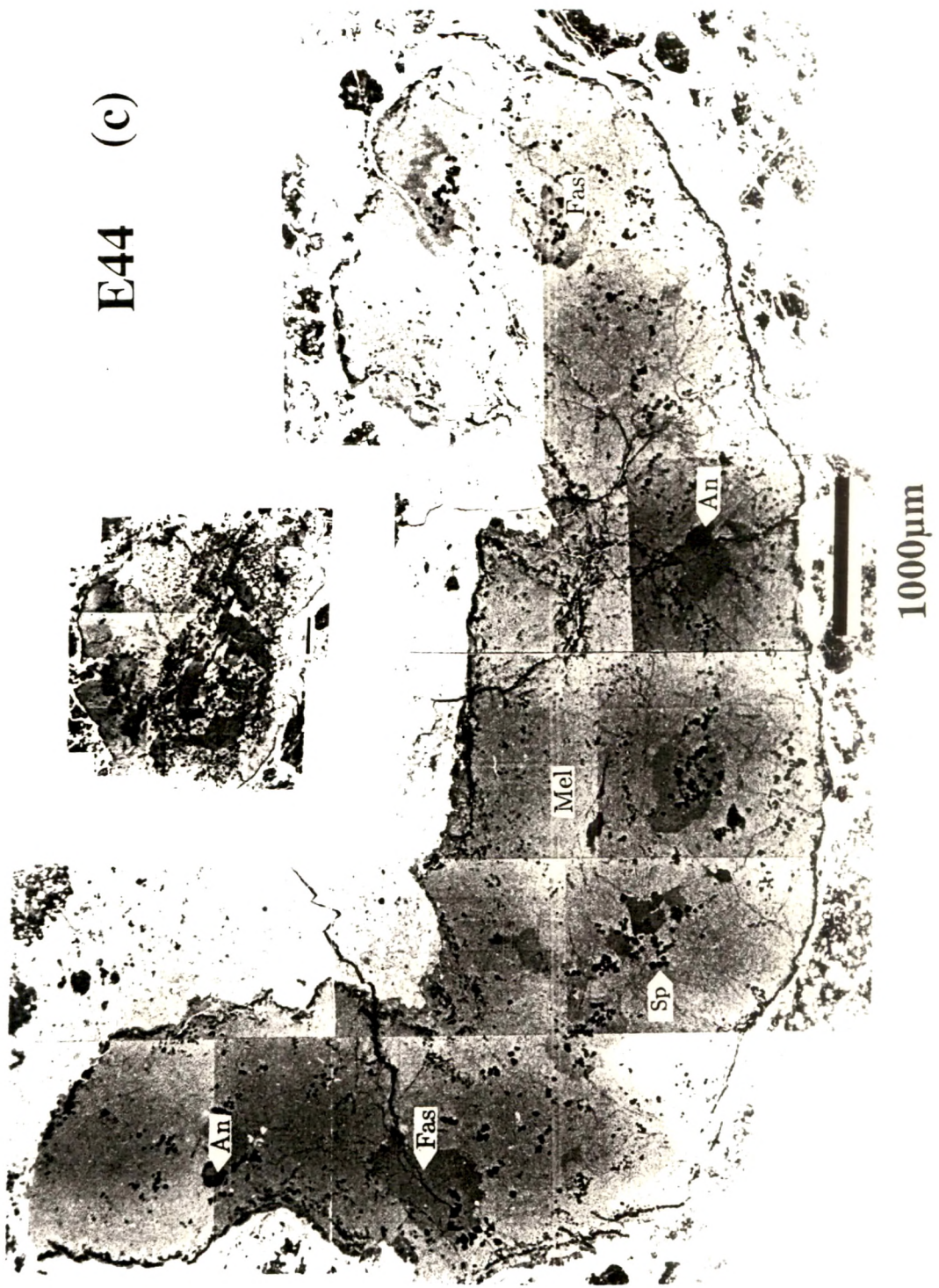


Fig.3.1 (Continued)

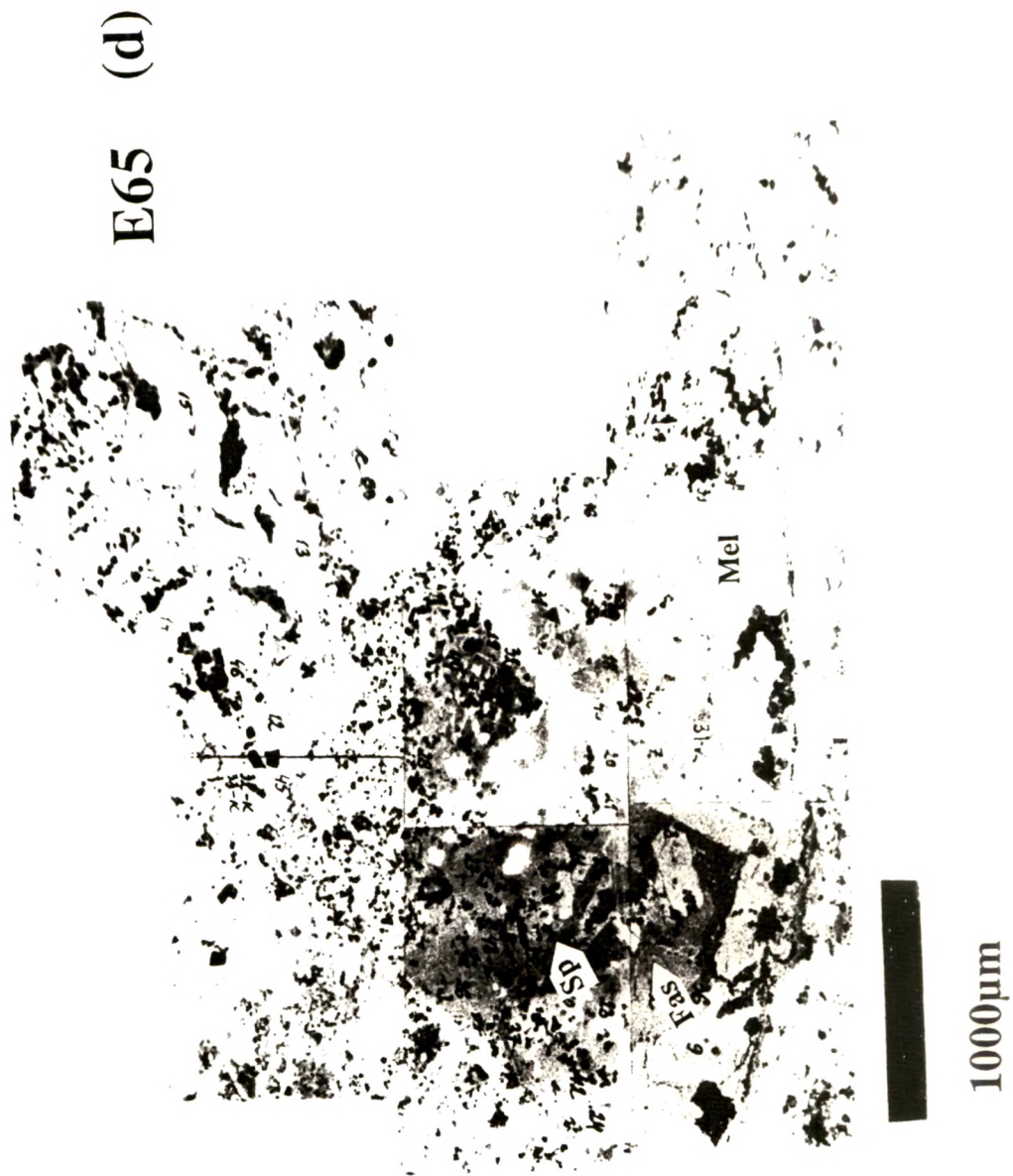


Fig.3.1 (Continued)





Fig.3.1 (Continued)

E36 (f)

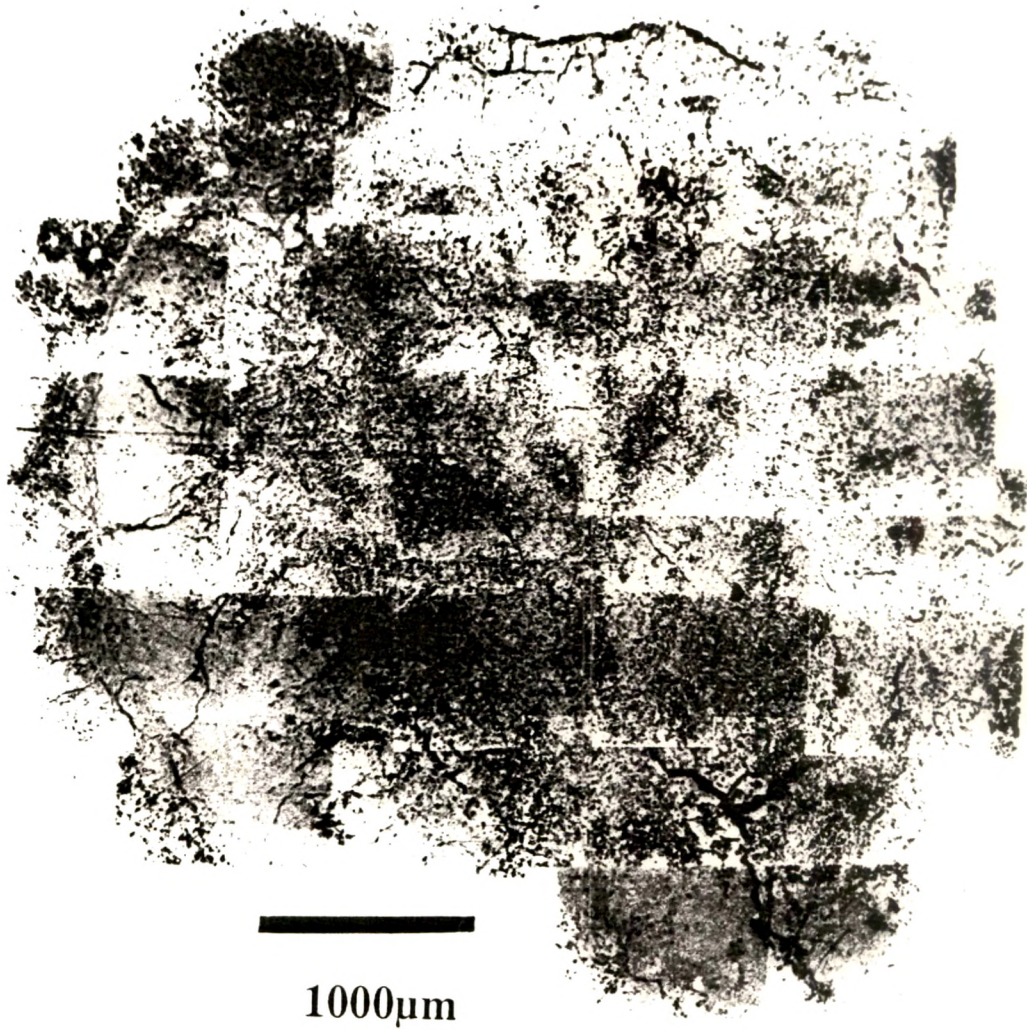


Fig.3.1 (Continued)

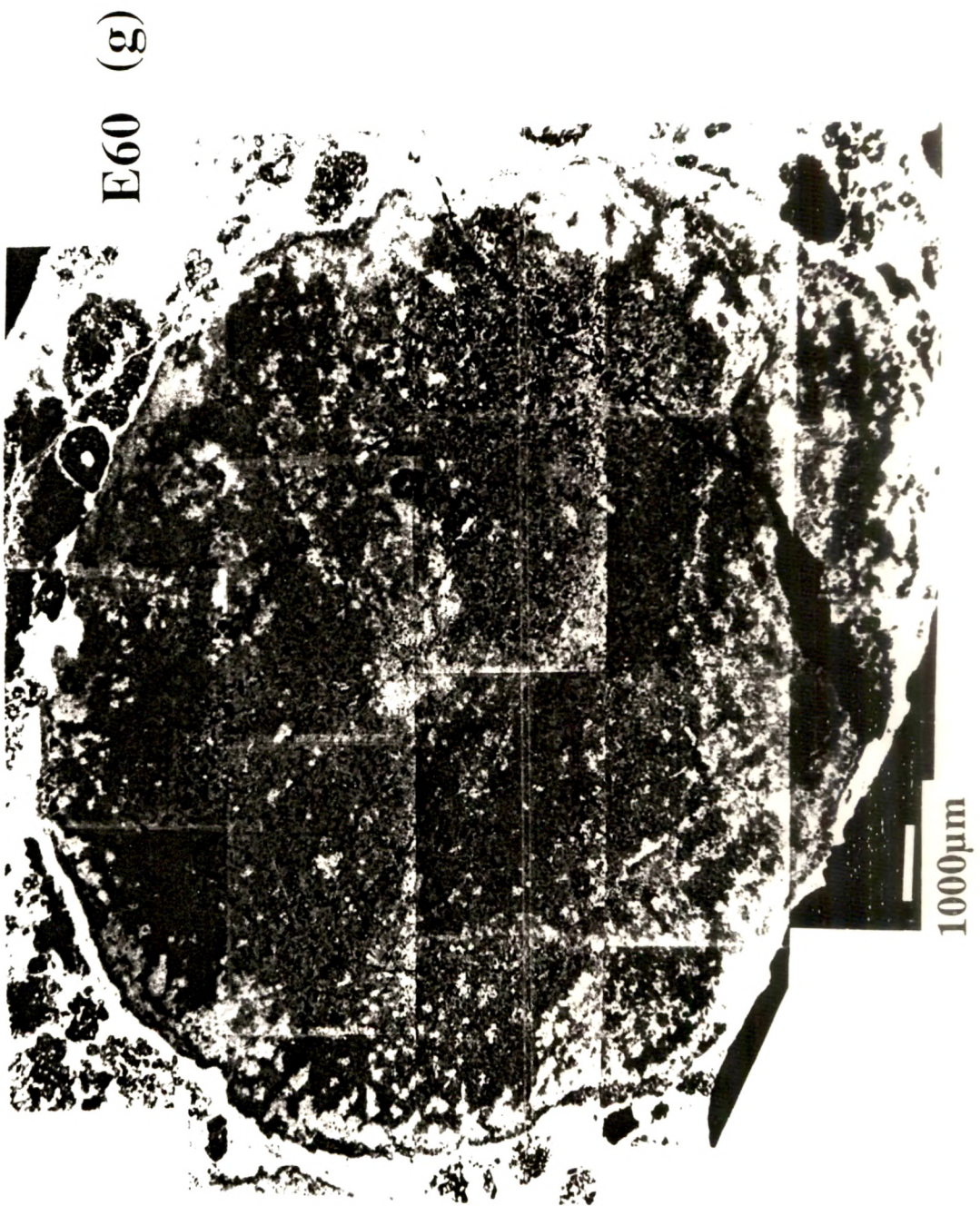
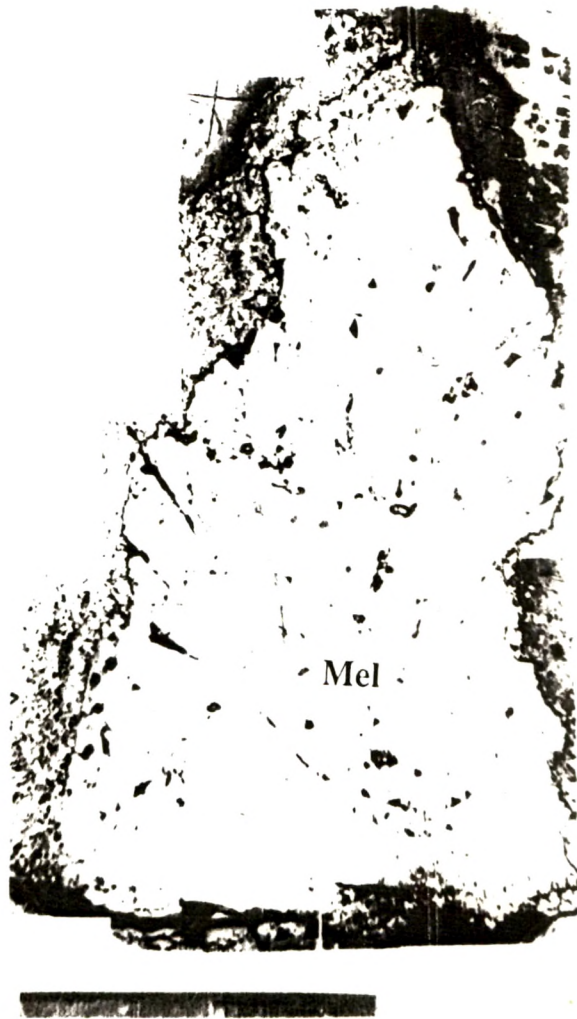


Fig.3.1 (Continued)

GR2 (h)



500µm

Fig.3.1 (Continued)

GR4 (i)

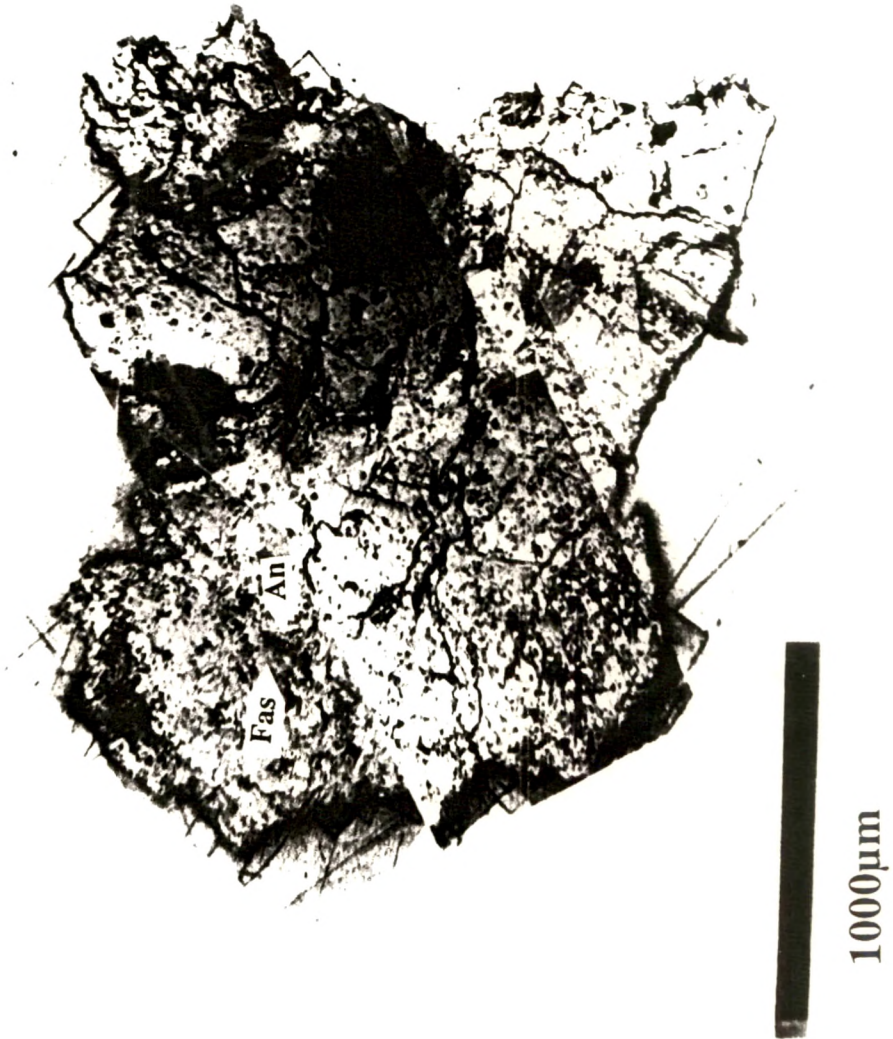


Fig.3.1 (Continued)

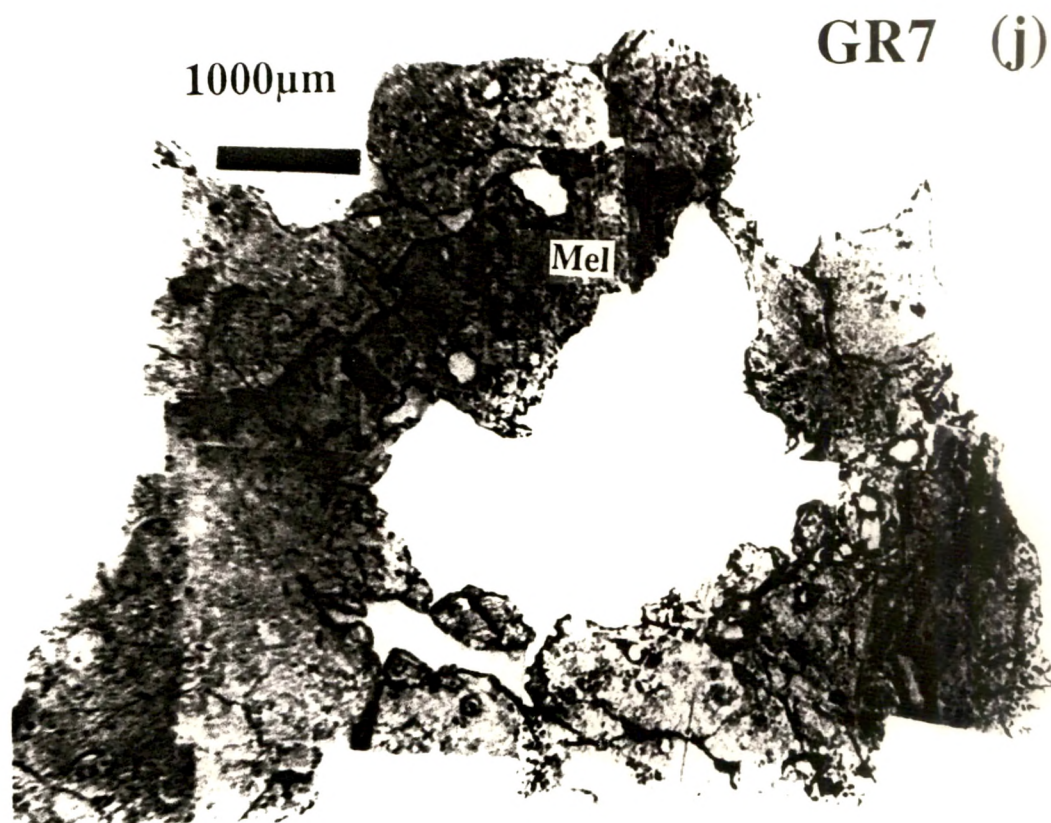


Figure 3.1: Optical photomicrograph of a polished section of Efremovka type A CAI E59, the dominant mineral phase is melilite. Backscattered electron photomicrographs of polished sections of the Efremovka type B1 CAIs E40 (b), E44 (c) and E64 (d). The E44 section analyzed represents a cut close to one of the edges of this CAI. A more representative cross section of E44 is shown as an inset in (c). The dominant mineral species are melilite, spinel and pyroxene can be easily identified. Anorthite present in E44 is marked. Backscattered electron photomicrograph of polished section of a Efremovka hibonite-rich CAI E50 (e). The dominant mineral phases are melilite, spinel and perovskite. Perovskite and hibonite rich zones are indicated. Optical photomicrograph and backscattered electron photomicrograph of polished sections of Efremovka type B2 CAIs E36 (f) and E60 (g). The dominant mineral phases are melilite and pyroxene. Optical photomicrographs of polished section of Grosnaja CAIs, type A GR2 (h), type C GR4 (i) and thin section of type B CAI GR7 (j). The dominant mineral phases are marked [ Melilite = Mel, Pyroxene = Fas, Spinel = Sp, Hibonite = Hib, Anorthite = An].

**Table 3.1: CAIs analyzed in this work**

<b>Petrographic type</b>	<b>Sample</b>
<b>Efremovka CAIs</b>	
type A	E2 and E59
type B1	E40, E44 and E65
type B2	E36 and E60
hibonite-rich	E50
<b>Grosnaja CAIs</b>	
type A	GR4
type B	GR7
type C	GR2

**Table 3.2: Composition of mineral phases in CAIs**

<b>Mineral</b>	<b>Composition</b>
<b>Primary Phases</b>	
Corundum	$\text{Al}_2\text{O}_3$
Hibonite	$\text{CaAl}_{12}\text{O}_{19}$
Perovskite	$\text{CaTiO}_3$
Spinel	$\text{MgAl}_2\text{O}_4$
Fassaite	$\text{Ca}(\text{Mg}, \text{Ti}, \text{Al})(\text{Al}, \text{Si})_2\text{O}_6$
Melilite	$\text{Ca}_2\text{MgSi}_2\text{O}_7$ - $\text{Ca}_2\text{Al}_2\text{Si}_7$
Anorthite	$\text{CaAl}_2\text{Si}_2\text{O}_8$
Diopside	$\text{CaMgSiO}_6$
<b>Secondary Phases</b>	
Grossular	$\text{Ca}_3\text{Al}_2\text{Si}_3\text{O}_{12}$
Nepheline	$\text{NaAlSiO}_4$
Sodalite	$\text{Na}_8\text{Al}_6\text{Si}_6\text{O}_{24}\text{Cl}_2$
Calcite	$\text{CaCO}_3$

**Table 3.3: Electron Microprobe Analysis of Melilite in Efremovka CAIs**

	E40(B1)		E44(B1)		E65(B1)		E60(B2)
	mantle	core	mantle	core	mantle	core	
SiO <sub>2</sub>	29.83	38.59	26.66	38.55	30.17	35	42.06
TiO <sub>2</sub>	0.06	0.02	-	-	0.02	0.01	-
Al <sub>2</sub> O <sub>3</sub>	23.79	10.85	29.01	10.80	25.14	17.09	4.76
Cr <sub>2</sub> O <sub>3</sub>	-	-	-	-	-	-	0.18
V <sub>2</sub> O <sub>3</sub>	-	-	-	-	-	-	0.11
CaO	41.17	40.89	41.43	40.41	39.94	40.68	39.31
MgO	4.18	9.81	2.78	10.16	4.96	7.84	13.09
FeO	0.03	0.02	0.01	-	0.03	0.16	0.28
MnO	-	-	0.09	0.02	-	-	-
Na <sub>2</sub> O	0.02	0.10	0.01	0.05	0.07	0.19	0.14
K <sub>2</sub> O	-	-	-	-	0.01	0.01	0.06
<b>SUM</b>	<b>99.08</b>	<b>100.28</b>	<b>100</b>	<b>100</b>	<b>100.34</b>	<b>100.98</b>	<b>99.99</b>

Note: "-" indicates no measurement



Table 3.4: Electron Microprobe Analysis of Pyroxene in Efremovka CAIs

	E65(B1)		E40(B1)		E44(B1)		E60(B2)	
	Low-Ti	High-Ti	Low-Ti	High-Ti	Low-Ti	High-Ti	Low-Ti	High-Ti
SiO <sub>2</sub>	45.39	39.75	42.23	37.41	44.68	35.17	52.24	33.99
TiO <sub>2</sub>	2.54	7.98	6.51	14.58	4.00	11.31	0.19	12.21
Al <sub>2</sub> O <sub>3</sub>	16.67	20.80	16.32	17.82	13.67	21.24	3.08	22.56
Cr <sub>2</sub> O <sub>3</sub>	0.05	0.06	0.10	0.06	0.03	-	-	-
V <sub>2</sub> O <sub>3</sub>	-	-	0.07	0.26	0.02	0.74	-	0.68
CaO	25.78	24.95	25.47	24.10	24.99	24.52	22.65	23.39
MgO	11.43	8.96	9.87	7.41	12.50	7.08	18.95	7.05
FeO	0.54	0.05	0.05	0.32	-	0.13	0.81	-
MnO	0.02	0.01	-	-	0.03	-	0.08	0.02
Na <sub>2</sub> O	0.06	-	-	0.03	0.08	-	-	0.07
K <sub>2</sub> O	0.02	0.01	0.01	-	-	-	-	0.03
SUM	102.50	102.57	100.63	101.72	100	100	98	100

Note: "-" indicates no measurement

Table 3.5: Electron Microprobe Analyses of Mineral Phases in E50

	Melilite	Hibonite	Perovskite	Spinel
SiO <sub>2</sub>	25.25	0.00	0.68	0.00
TiO <sub>2</sub>	0.02	7.25	56.76	0.24
Al <sub>2</sub> O <sub>3</sub>	31.94	79.81	1.09	69.63
FeO	0.08	0.00	0.04	0.58
MnO	0.00	0.00	0.11	0.00
MgO	2.33	4.73	0.05	28.99
CaO	40.24	7.92	41.09	0.17
Na <sub>2</sub> O	0.00	0.23	0.15	0.40
K <sub>2</sub> O	0.08	0.06	0.03	0.00
SUM	99.94	100.00	100.00	100.01

Table 3.6: Major element composition of mineral phases in Grosnaja CAIs

	GR2(Type C)				GR4 (Type A)				
	Anorthite	Pyroxene		Spinel	Garnet	Pyroxene	Melilite	Spinel	Garnet
		Core	Mantle						
SiO <sub>2</sub>	42.46	42.02	47.18	0.07	35.07	35.86	26.81	0.04	38.99
TiO <sub>2</sub>	0.08	5.16	2.50	0.38	0.01	9.55	0.03	0.35	0.01
Al <sub>2</sub> O <sub>3</sub>	36.44	14.42	9.72	70.53	0.04	21.64	28.83	71.78	22.79
Cr <sub>2</sub> O <sub>3</sub>	0.03	0.27	0.67	0.79	0.01	0.09	0.03	0.25	< 0.01
V <sub>2</sub> O <sub>3</sub>	< 0.01	0.16	0.13	0.33	< 0.01	0.15	0.01	0.41	0.01
MgO	0.11	11.76	13.31	27.36	0.17	7.53	3.20	28.02	2.45
CaO	20.04	25.59	25.49	0.08	33.43	25.28	41.10	0.16	34.93
FeO	0.10	0.16	0.21	0.53	28.26	0.02	0.08	0.08	1.35
MnO	0.01	< 0.01	0.04	0.02	0.01	< 0.01	0.01	0.03	0.02
Na <sub>2</sub> O	0.15	0.01	0.01	—	0.01	0.01	0.03	—	0.01
K <sub>2</sub> O	0.01	< 0.01	< 0.01	—	0.01	< 0.01	< 0.01	—	< 0.01

Note: All values are based on averages of 3 to 15 individual analysis